

SRBB-Based Quantum State Preparation

Giacomo Belli*

Marco Mordacci*

Michele Amoretti

Quantum Software Laboratory

University of Parma

Parma, Italy

{giacomo.belli,marco.mordacci1,michele.amoretti}@unipr.it

ABSTRACT

In this work, a scalable algorithm for the approximate quantum state preparation problem is proposed, facing a challenge of fundamental importance in many topic areas of quantum computing. The algorithm uses a variational quantum circuit based on the Standard Recursive Block Basis (SRBB), a hierarchical construction for the matrix algebra of the $SU(2^n)$ group, which is capable of linking the variational parameters with the topology of the Lie group. Compared to the full algebra, using only diagonal components reduces the number of CNOTs by an exponential factor, as well as the circuit depth, in full agreement with the relaxation principle, inherent to the approximation methodology, of minimizing resources while achieving high accuracy. The desired quantum state is then approximated by a scalable quantum neural network, which is designed upon the diagonal SRBB sub-algebra. This approach provides a new scheme for approximate quantum state preparation in a variational framework and a specific use case for the SRBB hierarchy.

The performance of the algorithm is assessed with different loss functions, like fidelity, trace distance, and Frobenius norm, in relation to two optimizers: Adam and Nelder-Mead. The results highlight the potential of SRBB in close connection with the geometry of unitary groups, achieving high accuracy up to 4 qubits in simulation, but also its current limitations with an increasing number of qubits. Additionally, the approximate SRBB-based QSP algorithm has been tested on real quantum devices to assess its performance with a small number of qubits.

KEYWORDS

Variational Quantum Circuit, State Preparation, Lie Algebra

1 INTRODUCTION

Quantum state preparation (QSP) is a very important step in many quantum algorithms, including various algorithms for quantum machine learning, quantum algorithms to solve systems of linear equations, and Hamiltonian simulation [16]. The goal of quantum state preparation is to construct a unitary operator U such that $|\psi\rangle = U|0\rangle^{\otimes n}$, where $|0\rangle^{\otimes n}$ is the n -qubit initial state and $|\psi\rangle = \sum_{i=0}^{2^n-1} c_i|i\rangle$ represents the desired quantum state in the computational basis, satisfying the complex normalization condition $\sum_{i=0}^{2^n-1} |c_i|^2 = 1$. Its approximate version aims to prepare a state $|\phi\rangle$ which is ϵ -close to $|\psi\rangle$ with respect to some metric. When defining quantum state preparation algorithms, whether to use ancillary qubits is another aspect that must be taken into consideration.

The study of QSP started in its exact version and without ancillary qubits with the method proposed by Nielsen and Chuang [34] (depth upper bound of $O(n^2)$). In the same period, while Grover and Rudolph [13, 14] proposed an algorithm for QSP in the special case of integrable probability density functions with a depth upper bound of $O(n2^n)$, Long and Sun [23] presented a scheme for arbitrary superpositions of the basis states, which required $O(n^22^n)$ 1-qubit and controlled gates. In 2004, Mottonen et al. [29] proposed a QSP algorithm exploiting uniformly controlled rotations [28], with a depth of $O(2^n)$ and $2^{n+2} - 4n - 4$ CNOT gates. Immediately after, Bergholm et al. [9] gave an upper bound of $2^{n+1} - 2n - 2$ for the number of CNOTs, with depth also of order $O(2^n)$, while Soklakov and Schack [46] obtained a very efficient algorithm for preparing sequences of states with suitably bounded amplitudes, following Grover's research line. In 2011, based on the universal gate decomposition proposed by Mottonen and Vartiainen [30, 48], Plesch and Brukner [37] focused on minimizing the CNOT count, achieving $\frac{23}{24}2^n - 2^{\frac{n}{2}+1} + \frac{5}{3}$ for even n , and $\frac{115}{96}2^n$ for odd n .

For the first time in 2016, Neimann et al. [35] introduced a synthesis approach to the QSP problem, deriving a methodology to automatically synthesize a circuit capable of generating any desired quantum state. Subsequently, Zhao et al. [56] proposed both deterministic and probabilistic state preparation based on quantum phase estimation, linking QSP to the decomposition of diagonal unitary operators [52]. In 2020, Mozafari et al. [31, 32] opened a research line on uniform QSP where scalability is ensured by the binary decision diagram and the decompositions made thanks to uniformly controlled rotations. Recently, Ramacciotti et al. [38] slightly modified the Grover-Rudolph algorithm for sparse quantum states, showing that the gate complexity is linear in the number of nonzero amplitudes and also in the number of qubits.

The use of ancillae in the history of QSP began with Zhang et al. [55], whose algorithm can generate the target state in $O(n^2)$ depth with $O(2^{2n})$ ancillary qubits, but only with a limited success probability. In the same year, Rosenthal [40] tackled the topic of space-time trade off by obtaining an algorithm with depth $O(n)$ using $O(n2^n)$ ancillary qubits. In 2022, Zhang et al. [54] presented another QSP circuit of depth $O(n)$ using $\Theta(2^n)$ ancillary qubits, but the asymptotically optimal space-time trade off bounds were found by Sun et al. [47] in their algorithm with depth $\tilde{O}(\frac{2^n}{m+n} + n)$ and width $O(2^n)$. The line of research culminated in the work of Yuan et al. [51]. Regarding the analysis of state preparation for sparse states with ancillae, a recent result was obtained by Luo et al. [25] with a systematic investigation of the circuit width.

*Both authors contributed equally to this research.

Narrowing the context, the following contributions should be highlighted within the field of Quantum Machine Learning, which seeks to utilize quantum computing to improve machine learning results in terms of performance and training efficiency [11]. A Quantum Neural Network (QNN) is a hybrid quantum-classical approach comprising a Variational Quantum Circuit (VQC) [7] and an optimization process performed using classical methods such as classical gradient descent. The VQC, which is the quantum counterpart of the classical neural network, is composed by a set of rotations whose angles are trained by the optimization process. In 2001, Kaye et al. [18] proposed a quantum network that is very efficient for generating pure symmetric states. Recently, Hai et al. [15] introduced a variational approach to QSP for entangled states, where the parametric ansatz has a hypergraph-based structure. The variational methodology was further developed by Wang et al. [50] with a noise-aware training which exploits back-propagation and incorporates real quantum noise into gradient calculations. The strategy of approximating the desired state by means of a parametric circuit is also used by Zhao et al. [57], while Gosset et al. [12] have recently published a study on the optimal number of T gates to approximate an arbitrary quantum state, improving previous work [24].

Other interesting works worthy of mention are the following ones. In 2019, Sanders et al. [41] presented a new algorithm for the class of black-box QSP that avoids the traditional Grover's arithmetic (which is a key contributor to complexity). The work of Romero et al. [39], Bondarenko et al. [10] and Zhang et al. [53] on quantum autoencoders (qae) poses interesting ideas for QSP, since once the qae has been trained, the decompression unitary can approximate the originally compressed states. Finally, Araujo et al. [3] proposed a combination of Möttönen's algorithm and a divide-and-conquer strategy to obtain an exponential speed up in the encoding processes.

As stated in its own definition, the problem of preparing the quantum state is closely connected with the topic of unitary synthesis (or gate synthesis), exact or approximate [4, 17, 21, 22, 44, 45, 49]. Recently, an approach to approximate synthesis based on Lie algebras [20] and classical optimization techniques was proposed [42, 43], based on the previous work of Madden and Simonetto [26]. The latter introduces a Hermitian unitary basis for the $\mathbb{C}^{2^n \times 2^n}$ algebra, called the Standard Recursive Block Basis (SRBB), to obtain a scalable and recursive representation for any unitary operator. Subsequently, the scalable structure of the SRBB-based unitary decomposition was used to design the VQC of a quantum neural network for approximate synthesis tasks, optimized in terms of CNOTs, and tested both in simulation and with a real quantum computer [5, 6].

This paper provides the following new contributions: 1) a novel approximate QSP algorithm is proposed, as a specific use case of the SRBB hierarchy; 2) the traditional ladder structure of QSP circuits is implemented with only the CNOT-optimized diagonal SRBB sub-algebra, so as to reduce its depth, approaching the asymptotically optimal bounds of Sun et al. [47]; 3) the algorithm's performance is assessed with random states, sparse states, and states with a uniform probability distribution, up to 8 qubits; 4) the QNN is also tested with real quantum devices (provided by IQM [36]) to assess

its performance in a real environment with random states and specific states, such as Bell and GHZ.

The remainder of the paper is organized as follows. In Section 2, the *Standard Recursive Block Basis* is presented, focusing on its diagonal sub-algebra represented by the $Z(\Theta_Z)$ -factor. This theoretical framework based on Lie algebras is then contextualized in the problem of state preparation, analyzing different possible implementation strategies related to the QSP natural structure of uniformly controlled gates. In the last part of the section, it is shown, also through examples, how to build a scalable QSP circuit using only the SRBB Z -factor, S and H gates. Then, formulas for depth and gate count are provided. In Section 3, the implementation of the corresponding QNN is explained in detail. In addition, the results obtained in simulation and with real quantum devices are presented with a related description. Finally, Section 4 concludes the paper with a summary of the main results and a discussion of future work.

2 THEORETICAL FRAMEWORK

The *Standard Recursive Block Basis* (SRBB) [43] is the hierarchical and recursive construction that defines for any $n \in \mathbb{N}_+$ the Hermitian unitary basis of the $\mathbb{C}^{2^n \times 2^n}$ matrix algebra. Originally introduced to obtain a scalable parameterized representation of unitary matrices, it can be thought of as a generalization of the Pauli basis for complex matrices of higher orders. Accordingly, any unitary operator can be expressed as a product of exponentials of SRBB elements, ordered according to a specific algebraic criterion, thanks to the properties of the connected topological space that characterizes the Lie group $U(2^n)$.

Since $U(d) = U(1) \times SU(d)$, any unitary matrix is a phase scaling of d special unitary matrices; thus, any $U = e^{i\alpha}V$ where $\det(V) = 1$, satisfies $\det(U) = e^{i\alpha \cdot d} \det(V) = e^{i\alpha \cdot d}$ leading the determination of the rescaling phases to the resolution of equations of degree $d = 2^n$ on the complex plane. Therefore, for any $U \in U(d)$, it holds that $\frac{U}{[\det(U)]^{\frac{1}{d}}} \in SU(d)$. This fact allows, first of all, to work only with SRBB elements that build the special unitary sub-algebra without losing generality and, secondly, to define a phase correction approach to the learning process of the QNN for approximate synthesis tasks concerning $U(d)$.

The SRBB elements $U_j^{(d)}$, where $1 \leq j \leq 2^n$, become the building blocks of a scalable unitary synthesis algorithm capable of approximating any given $U \in SU(2^n)$ according to [43]:

$$U_{approx} \equiv \prod_{l=1}^L Z(\Theta_Z^l) \Psi(\Theta_\Psi^l) \Phi(\Theta_\Phi^l) \quad (1)$$

where l is the layer index, indicating the number of repetitions of the approximating scheme depicted in Figure 1. The SU sub-algebra of SRBB is partitioned into three subsets according to the algebraic properties of its matrix elements $U_j^{(d)}$ and then used to define each macro-factor of equation (1), in turn represented by the variational blocks of Figure 1. The QSP algorithm presented in this work only uses the diagonal Z -factor, defined by the following equation ($l = 1$):

$$Z(\Theta_Z) = \prod_{j=2}^{2^n} e^{i(\theta_{j^2-1} U_{j^2-1}^{(2^n)})} \quad (2)$$

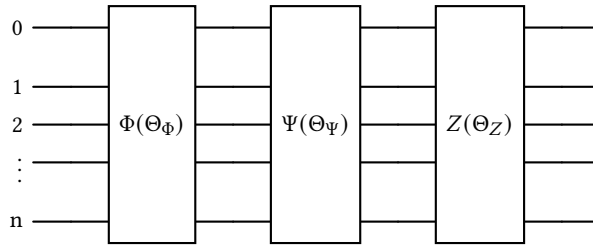


Figure 1: VQC for approximating $SU(2^n)$ operators with one single layer.

where $U_{j^2-1}^{(2^n)}$ are diagonal SRBB elements and θ_{j^2-1} are the corresponding variational parameters. This factor can describe any *diagonal* SU operator, thus a diagonal matrix of pure complex phases with unit determinant. Defining the role of each macro-factor is useful for understanding why it is convenient to work with only the diagonal component of the algebra in order to reduce the overall depth of the traditional QSP circuit (Figure 2a) so as to approach the optimum achieved by [47], but without the use of ancillae. The Ψ -factor is made up by SRBB elements which already admit by construction a ZYZ -decomposition (so they belong to the group M_nZYZ) and by other elements which instead admit the same decomposition only after the application of transposition matrices¹ of even indices (which is why they are called even contributions). Therefore, Ψ -factor can describe any $SU(2)$ -block diagonal matrix belonging to $SU(2^n)$. Conversely, the Φ -factor is made up of SRBB elements which admit a *partial* ZYZ -decomposition only after the application of transposition matrices of odd indices (and so they are called odd contributions). Therefore, the Φ -factor can describe any $U(2)$ -block diagonal matrix belonging to $SU(2^n)$.

In [6], the SRBB synthesis algorithm was transferred into a quantum context through the scalable design of the corresponding VQC and a new CNOT-reduced scalability scheme was identified and implemented with one single layer ($l = 1$). Subsequently, the corresponding QNN was tested in both simulation and real quantum hardware [5], to establish the effectiveness of the SRBB hierarchy in approximate synthesis tasks. The SRBB creates a direct connection between the topology of the special unitary group and the matrix algebra capable of representing unitary operators recursively, allowing the design of scalable variational algorithms. How to leverage this link to design a state preparation algorithm with competitive depth trends and at the same time define a specific use case for SRBB? This question was the research motivation for this work.

According to the QSP paradigm, if the starting algebraic basis were complete SRBB, any unitary (and therefore any state) could be represented parametrically. However, thanks to the relationship that exists between the Lie groups $U(2^n)$ and $SU(2^n)$, it is sufficient to construct a parametric ansatz describing the arbitrary SU operator. In fact, the discrepancy between the final states would only consist of a global phase, irrelevant in the experimental (real hardware) evaluation of the desired state or easily implementable with a few

¹Transpositions, or 2-cycles, are elements of the Permutation group P_{2n} with $2^n - 2$ fixed point.

single-qubit gates². At this point, if the natural framework for QSP is considered [29], which involves a ladder structure of uniformly controlled gates (UCGs) throughout the quantum register as shown in Figure 2a, each factor of the SRBB-based synthesis algorithm could have its own role. In fact, in matrix form, UCG is a block-

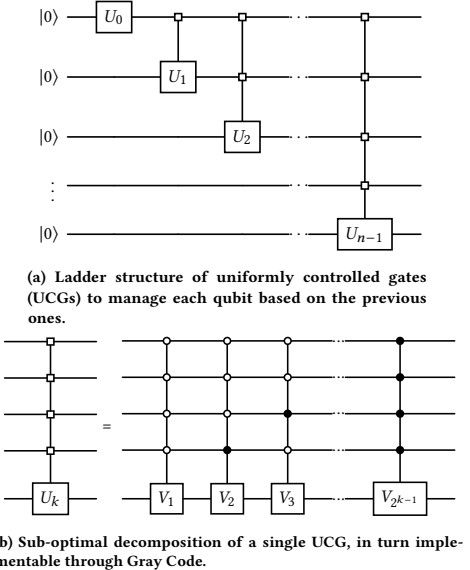


Figure 2: QSP natural framework.

diagonal operator $U_k = \text{diag}(V_1, V_2, \dots, V_{2k-1}) \in \mathbb{C}^{2^k \times 2^k}$, where each block $V_i \in U(2)$, therefore representable through $\Phi(\Theta_\Phi)$ -factor alone. In this case, for each UCG of the QSP circuit, a sub-circuit with $5 \cdot 2^{n-1} - 6$ CNOT gates would be required [43]. If, instead, the UCG was restricted to the case of special unitary blocks $V_i \in SU(2^n)$, then it would be representable by the $\Psi(\Theta_\Psi)$ -factor alone and the number of CNOTs for each controlled gate would go down to $3 \cdot 2^{n-1} - 2$.

So long as the total number of CNOTs required in the Z -factor scaling scheme is $2^n - 2$ [5], it would be much better to be able to exploit only the diagonal sub-algebra and thus reduce the overall circuit depth. However, this approach is not compatible with the natural framework of QSP and the UCGs contained therein, because the Z -factor parametrizes only diagonal unitary matrices, the entries of which are complex phases. One result can provide a variational approach to QSP that uses the SRBB diagonal sub-algebra while maintaining the traditional structure: each unitary matrix $V_i \in U(2)$ can be decomposed in terms of S , H and R_z gates [47], according to the well known identity

$$R_y(\gamma_i) = SH \cdot R_z(\gamma_i) \cdot HS^\dagger \quad (3)$$

such that $V_i = e^{i\alpha_i} R_z(\beta_i) S H R_z(\gamma_i) H S^\dagger R_z(\delta_i)$. In addition, the implementation of the Ψ - and Φ -factors of SRBB exploits a Gray Code pattern equivalent to the decomposition of an arbitrary multiplexor or UCG (see Figure 2b), resulting in alternating sequences of CNOT,

²A diagonal unitary matrix with entries equal to $e^{i\phi}$, for some $\phi \in \mathbb{R}$, can be added to the quantum circuit thanks to the combination $R_z(2\phi) \cdot X R(2\phi) X$, where X is the Pauli gate and R is the Phase Shift gate.

R_z and R_y gates [5, 43]. Therefore, diagonal unitary matrices can encode the information of a UCG if their parameters are chosen appropriately and with the help of single qubit gates, like S and Hadamard, a fact that allows to design a scalable QSP algorithm with only the diagonal component of the SRBB algebra.

2.1 QSP natural structure

For a n -qubit system, a state preparation algorithm aims to prepare any desired quantum state $|\psi\rangle = \sum_{i=0}^{2^n-1} c_i |i\rangle$, where $c_i = |c_i| e^{i\phi_i}$ are the amplitudes associated with the vector $c = (c_0, c_1, c_2, \dots, c_{2^n-1}) \in \mathbb{C}^{2^n}$ with unit l_2 -norm, eventually random. The QSP natural framework consists of a ladder structure of uniformly controlled gates (UCGs), as illustrated in Figure 2a, where each qubit k is handled by an UCG which has the task of applying a single qubit unitary on it, conditioned on the basis state of the first $k-1$ qubits. When defining the UCG to be included in the general structure, without losing generality, it is possible to consider $SU(2)$ blocks like $R_y(\theta)$, thus greatly simplifying the algorithm and its implementation. An exact QSP algorithm must find the best way to implement each UCG, since the usual decomposition³ shown in Figure 2b is sub-optimal, as proven in [47]. Whether it is an exact or approximate QSP, the multiplexor structure in Figure 2a requires a classical step to determine the UCG parameters necessary to achieve the desired state $|\psi\rangle$. The latter task can be performed thanks to the Binary Search Tree (BST), a diagram that stores the amplitudes c_i of the desired state $|\psi\rangle$ in its leaf nodes (see Figure 3). Every internal node

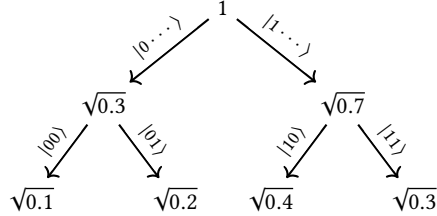


Figure 3: Binary Search Tree for the complex amplitudes of the desired state.

stores the square root of the sum of squares of its child nodes, and the root node stores the l_2 -norm of the vector c . Moreover, it is necessary to consider the traditional decomposition of a UCG, based on its own definition, illustrated in Figure 2b. In the following, the $n=2$ case exemplifies this classical step characterizing the natural structure of the QSP problem.

2.1.1 Finding parameters for $n=2$. According to the natural framework, the fully decomposed quantum circuit to prepare an arbitrary state with 2 qubits is depicted in Figure 4. As anticipated, the choice of R_y -blocks allows us to simplify the classical determination of the natural parameters (the ones associated to the natural decomposition of Figure 2b). While in exact QSP this step is mandatory because these parameters have to coincide with the new ones of the equivalent, and preferably better implemented, circuit (see, for instance, [47]), in its relaxed version they represent the ideal target

³The decomposition of a multiplexor in the complete sequence of controlled gates allows the further implementation through a cyclic Gray Code.

set of parameters that the variational approach must approximate. With reference to the BST illustrated in Figure 3, the parameter θ_0

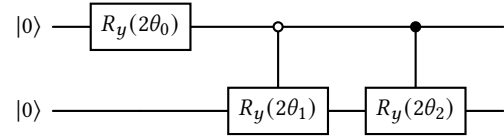


Figure 4: QSP traditional circuit for $n=2$.

associated with $U_0 = R_y(2\theta_0)$ is derived considering that U_0 acts only on the first qubit initialized in $|0\rangle$. Thus, $\theta_0 = \arccos \sqrt{\frac{0.3}{1}}$. Similarly, the parameters θ_1 and θ_2 are derived considering that U_1 and U_2 act, respectively, when the quantum state of the register is $|00\rangle$ or $|10\rangle$, leading to $\theta_1 = \arccos \sqrt{\frac{0.1}{0.3}}$ and $\theta_2 = \arccos \sqrt{\frac{0.4}{0.7}}$. Obviously, not all nodes of the BST (and, therefore, not all amplitudes) influence the circuit parameters; some of them are indirectly considered by the normalization condition present at each level of the BST. In a matrix representation, the quantum circuit is equivalent to:

$$\begin{aligned} & \text{UCG}_2(2\theta_1, 2\theta_2) \cdot [R_y(2\theta_0) \otimes \mathbb{I}_2] |0\rangle^{\otimes 2} = \\ &= \begin{pmatrix} \cos \theta_1 \cos \theta_0 & -\sin \theta_1 \cos \theta_0 & -\cos \theta_1 \sin \theta_0 & \sin \theta_1 \sin \theta_0 \\ \sin \theta_1 \cos \theta_0 & \cos \theta_1 \cos \theta_0 & -\sin \theta_1 \sin \theta_0 & -\cos \theta_1 \sin \theta_0 \\ \cos \theta_2 \sin \theta_0 & -\sin \theta_2 \sin \theta_0 & \cos \theta_2 \cos \theta_0 & -\sin \theta_2 \cos \theta_0 \\ \sin \theta_2 \sin \theta_0 & \cos \theta_2 \sin \theta_0 & \sin \theta_2 \cos \theta_0 & \cos \theta_2 \cos \theta_0 \end{pmatrix} \begin{pmatrix} 1 \\ 0 \\ 0 \\ 0 \end{pmatrix} = \\ &= \begin{pmatrix} \cos \theta_1 \cos \theta_0 \\ \sin \theta_1 \cos \theta_0 \\ \cos \theta_2 \sin \theta_0 \\ \sin \theta_2 \sin \theta_0 \end{pmatrix} = \begin{pmatrix} \sqrt{0.1} \\ \sqrt{0.2} \\ \sqrt{0.4} \\ \sqrt{0.3} \end{pmatrix} \end{aligned} \quad (4)$$

The choice $V_i = R_y(2\theta_i)$ simplifies the determination of the parameters of the quantum circuit but, as shown by equation 4, produces a completely real output vector, whose components correspond to $|c_i|$, the modulus of the complex amplitudes of the desired vector $|\psi\rangle$. Indeed, from an experimental point of view (real hardware), a QSP algorithm must determine the probability distribution of the basis states of the quantum register corresponding to the desired quantum state, leaving out the information contained in the phases that is destroyed by the measurement process. However, by extending the domain of applicability of a QSP algorithm to the *Encoding* process, it is important to also take into account the whole complex amplitude c_i , at least when the output of a QSP circuit is the input of another algorithm. In the next section, a part of the variational quantum circuit will be dedicated to that, and once again only the Z -factor of the SRBB will be needed.

2.2 VQC for the diagonal SRBB hierarchy

In [6], a novel scalability scheme optimized in terms of CNOT gates is obtained for the diagonal components of the SRBB matrix algebra. As a result, the Z -factor can be easily implemented thanks to a partially recursive structure made up of two main blocks in which CNOTs and R_z gates alternate. The circuit-level Z -factor construction algorithm involves sorting the diagonal elements of the algebra into a matrix of binary strings that represent the numbers from 1 to $2^n - 1$. For each n , the aforementioned binary table presents some new algebraic contributions of the case under consideration

(binary strings ending with 1) and others of the case $n-1$ (binary strings ending with 0). It has been demonstrated [5] that the new contributions of the case n can be ordered to minimize the number of CNOTs via cyclic Gray Code matrices, while the old ones can be incorporated into the implementation of the case $n-1$. This is true except for the $n=2$ case, which falls outside the scalability scheme as the minimum number of qubits to have non-trivial SRBB and therefore the starting point of the recursion. The sequence of rotation angles is defined by the same Gray Code matrix that encodes the optimization of the CNOTs. A detailed analysis of the CNOT optimization and the complete description of the resulting scalable algorithm for the Z-factor can be found in [5]; Figure 5 exemplifies this scalable structure for the $n=3$ case.

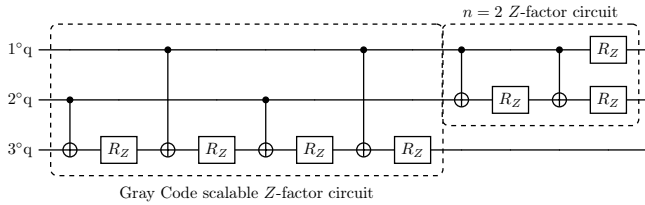


Figure 5: The $Z(\Theta_Z)$ -factor circuit for $n=3$ with reduced CNOT-count.

2.2.1 *Implementing R_y -block UCGs.* According to identity (3), an arbitrary UCG U_k only composed by R_y blocks and with $\Theta_k = (\theta_1, \theta_2, \dots, \theta_{2^{k-1}})$ admits the following decomposition in terms of multi-controlled R_z -gate:

$$\begin{aligned} U_k = & [\mathbb{I}_{n-1} \otimes (SH)] \cdot \\ & \cdot \text{diag}[R_z(\theta_1), R_z(\theta_2), \dots, R_z(\theta_{2^{k-1}})] \cdot \\ & \cdot [\mathbb{I}_{n-1} \otimes (HS^\dagger)] \end{aligned} \quad (5)$$

in such a way that at the circuit level the substitution illustrated in Figure 6 occurs. Therefore, the QSP ladder structure of Figure 2a

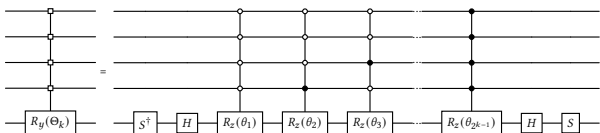


Figure 6: R_y -block UCG circuit.

can be redesigned with only gates S , H and R_z , a configuration that is formally equivalent to a sequence of diagonal unitary matrices of pure complex phases and thus representable through the diagonal SRBB sub-algebra. Figure 7 shows the case $n=3$, where the circuit blocks that can be approximated by the Z-factor of the SRBB are highlighted with a dotted line. A final circuit block consisting of $Z_{n_{max}}^{SRBB}$ has been added to the original scale structure and separated by a dotted line; the latter encodes the necessary phase correction after choosing to consider only the R_y blocks in the UCGs, as explained in Section 2.1.1.

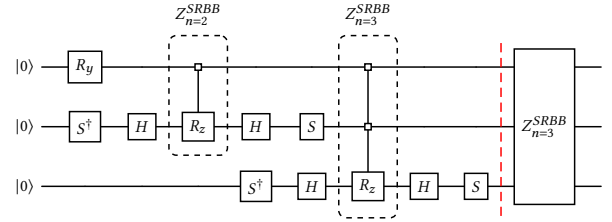


Figure 7: QSP circuit with insertions for the Z-factor in the $n=3$ case. The barrier separates the component that learns the moduli from the one that learns the phases.

2.2.2 *Depth and gate counts.* The depth trend and gate count as a function of the number of qubits n can easily be deduced by following the recursive structure given by the Z-factor to the overall circuit.

Since the recursive structure is valid from $n \geq 3$, we keep aside the contribution to the depth given by the R_y on the first qubit and by the first UCG₂⁴, a contribution which is equal to $2+Z_{n=2}^{SRBB}+2=8$. As can be seen in Figure 7, at every $n \geq 3$ the S^\dagger and H gates do not create depth as they are parallel to the circuit for Z_{n-1}^{SRBB} . The same happens for the gates H and S following the implementation of Z_n^{SRBB} . This implies that from $n \geq 3$, the depth is given only by the Z-factors up to n_{max} , as stated by the following equation:

$$D(n_{max}) = 8 + \sum_{n=3}^{n_{max}} \mathcal{Z}_n + \mathcal{Z}_{n_{max}} \quad (6)$$

where \mathcal{Z}_n represents the contribution of each Z_n^{SRBB} factor according to

$$\mathcal{Z}_n = \sum_{i=3}^n (2^i - 1) + 4 = 2^{n+1} - 2 - n \quad (7)$$

Thus, for $n_{max} = M$, it holds that

$$\begin{aligned} D(M) = & 8 + \sum_{n=3}^M (2^{n+1} - 2 - n) + 2^{M+1} - 2 - M = \\ & = 2^{M+2} - 2M - 4 - \Delta_{3,M} + 2^{M+1} - 2 - M \end{aligned} \quad (8)$$

where $\Delta_{3,M}$ represents the sum of the integers from 3 to M , obtained from the well known Euler's formula $S_{n_1 \rightarrow n_2} = \frac{n_2(n_2+1)-n_1(n_1+1)}{2} + n_1$, for $n_1 < n_2$. Substituting into the previous equation, the depth trend as function of the number of qubits n becomes:

$$D(n) = 6 \cdot 2^n - \frac{n^2 + 7n}{2} - 3 \quad (9)$$

Finally, for each Z_n^{SRBB} for $n \geq 3$, the number of CNOTs is equal to $2^n - 2$ while the number of R_z is equal to $2^n - 1$. Following a similar reasoning to that of depth, the total number of rotations is:

$$\begin{aligned} N_{rot}(n) = & 4 + \mathcal{Z}_n^{rot} + 2^n - 1 = \\ & = 3 \cdot 2^n - n - 3 \end{aligned} \quad (10)$$

where

$$\mathcal{Z}_n^{rot} = \sum_{i=3}^n (2^i - 1) = 2^{n+1} - n - 6 \quad (11)$$

⁴With the symbol UCG_n is indicated the multiplexor upon n qubits.

The total number of CNOT gates can be computed as:

$$N_{CNOT}(n) = 2 + \mathcal{Z}_n^{CNOT} + 2^n - 2 = 3 \cdot 2^n - 2n - 4 \quad (12)$$

where

$$\mathcal{Z}_n^{CNOT} = \sum_{i=3}^n (2^i - 2) = 2^{n+1} - 2n - 4 \quad (13)$$

3 QNN IMPLEMENTATION AND RESULTS

The proposed VQC has been implemented using the PennyLane library [8]. The tests have been performed using the simulator provided by the library, executed on a Linux machine equipped with an AMD EPYC 7282 CPU and 256 GB RAM, and real IQM quantum computers, namely IQM Deneb and IQM Garnet.

Figure 8 provides a general depiction of the QNN, which is used to prepare the desired state and operates in two steps, as indicated by the barrier in Figure 7 with 3 qubits:

- (1) the first part of the network learns the modulus of each component of the desired state;
- (2) the second part of the network learns how to produce the phase for each component of the desired state.

When the VQC has to learn the moduli of the state, the unitary $U_{Modulus}$ associated to the QSP natural structure is calculated following Section 2.1 and then approximated by the first part of circuit in Figure 7. On the other hand, when the VQC has to learn the phases, the target unitary U_{Phase} is a diagonal matrix, whose diagonal elements are defined as the complex phases of each amplitude of the desired state. Subsequently, the $2^n SU_{Phase}$ matrices related to U_{Phase} must be calculated, as the Z-factor employed in the implementation of the second part of the circuit in Figure 7 can only represent SU operators (Section 2.2), so it must learn one of these SU , using the same technique introduced in Remark 1 of Section 2 in [5]. Training of these two components cannot be simultaneous, as it would prevent the network from distinguishing which part is responsible for each task, making it a more difficult task, and therefore hindering the network's ability to correctly learn the circuit. At the end of the training, the resulting network will generate the exact state up to a global phase. In any case, this issue can be corrected in U_{Phase} by multiplying the unitary matrix by the root of the determinant of the corresponding SU , as explained in Remark 1 of Section 2 in [5]. Alternatively, if the correction has to be applied directly to the quantum circuit, the global phase can be added to the diagonal elements by applying a unitary operation to one qubit, consisting of the gate sequence $R_z(2\phi) \cdot PauliX \cdot PhaseShift(2\phi) \cdot PauliX$, where ϕ is the global phase and:

$$PhaseShift(\phi) = \begin{pmatrix} 1 & 0 \\ 0 & e^{i\phi} \end{pmatrix} \quad (14)$$

$$R_z(\phi) = \begin{pmatrix} e^{-i\frac{\phi}{2}} & 0 \\ 0 & e^{i\frac{\phi}{2}} \end{pmatrix} \quad (15)$$

All results from the real quantum computers (Section 3.2) have been obtained using the original circuit, without correcting the global phase, as the objective is to assess the performance of the algorithm. Moreover, the error has been computed by calculating the Hellinger distance between the target probabilities and those

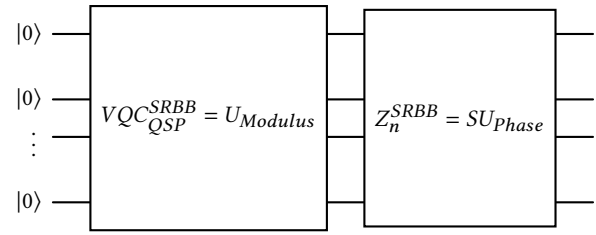


Figure 8: General structure of the QNN, divided in the two component: $U_{Modulus}$, which learns the moduli of the state, and SU_{Phase} , which learns the phases.

produced by the network. Therefore, the global phase does not affect the results.

Different loss functions are tested:

- Frobenius norm: $\|A\|_F = \sqrt{\text{tr}(AA^\dagger)}$, where $A = SU_{ideal} - SU_{VQC}$
- Trace distance: $\|\rho - \sigma\|_1 = \text{tr} \sqrt{(\rho - \sigma)^\dagger (\rho - \sigma)}$
- Fidelity: $F(\rho, \sigma) = \left(\text{tr} \sqrt{\sqrt{\rho} \sigma \sqrt{\rho}} \right)^2$, where ρ and σ are the density matrices of the states obtained by the ideal SU or U operation, which will be approximated, and by the VQC, respectively, given the same input state.

When the Frobenius norm is used as the loss function, the VQC is designed to obtain its matrix representation. The Frobenius distance is then calculated to evaluate the loss. This approach involves comparing the $SU(2^n)_{Phase}$ or $U(2^n)_{Modulus}$ matrix associated with the target circuit that the QNN aims to approximate and the $SU(2^n)_{Phase}$ or $U(2^n)_{Modulus}$ matrix associated with the VQC.

On the other hand, when one among fidelity or trace distance is used as the loss function, a training set of 1000 random states is generated. The loss function is minimized by adjusting the VQC to decrease the trace distance (or increase the fidelity) between the states produced by the ideal matrix and those obtained from the approximated matrix.

Two different optimizers are used based on the chosen loss function:

- Adam [19]: used with trace and fidelity, with learning rate 0.01, 50 epochs and batch size 64;
- Nelder Mead [33]: used with Frobenius, with 10^{-15} as objective error with 2 and 3 qubits, while 10^{-10} with 4 qubits, otherwise the training time becomes excessively long.

3.1 Quantum Circuit Simulation

The QNN has been tested with different numbers of qubits, from 2 to 8, with random states but also specific states, such as Bell, GHZ and uniform superposition. The mean results are shown in Table 1. The error is computed as the trace distance between the target state and the state achieved by the network.

The Nelder Mead optimizer demonstrates effective performance up to 4 qubits. However, when the circuit has to approximate 4-qubit states, the accepted error has been decreased from 10^{-15} to 10^{-10} to achieve the approximation in an acceptable time, as shown in

the table. As the number of qubits increases, the problem becomes more complex and the optimizer cannot converge effectively.

On the other hand, the Adam optimizer exhibits longer training times for fewer qubits, but these do not increase exponentially. Furthermore, when the fidelity is used as a loss function, the network's results closely match the results achieved with Nelder Mead. Moreover, the network can also approximate states with higher amplitude. Conversely, using trace distance as the loss function significantly diminishes the network's performance compared to the other metrics.

n qubit	Time taken with Adam	Error with Adam + fidelity	Error with Adam + trace distance	Time taken with Nelder Mead	Error with Nelder Mead
2	$\sim 9m$	$\sim 10^{-15}$	$\sim 10^{-3}$	$\sim 2s$	$\sim 10^{-15}$
3	$\sim 16m$	$\sim 10^{-13}$	$\sim 10^{-3}$	$\sim 30s$	$\sim 10^{-15}$
4	$\sim 33m$	$\sim 10^{-13}$	$\sim 10^{-3}$	$\sim 9m$	$\sim 10^{-10}$
5	$\sim 1h$	$\sim 10^{-7}$	$\sim 10^{-3}$	—	—
6	$\sim 2h$	$\sim 10^{-3}$	$\sim 10^{-3}$	—	—
7	$\sim 5h$	$\sim 10^{-3}$	$\sim 10^{-3}$	—	—
8	$\sim 11h$	$\sim 10^{-3}$	$\sim 10^{-3}$	—	—

Table 1: Results achieved in simulation from 2 to 8 qubits.

3.2 Real Quantum Computers

This section presents the results obtained from running the trained VQC (with fidelity as loss function) on real quantum computers. Specifically, the experiment was carried out using the following 2 quantum computers, provided by IQM:

- IQM Garnet. It is a 20-qubit quantum processing unit based on superconducting transmon qubits. The qubits are arranged in a square lattice and connected by tunable couplers. The system is calibrated to support arbitrary X and Y rotations as the native single-qubit gate and CZ as the native two-qubit gate [1].
- IQM Deneb. It is a 6-qubit quantum processing unit where all superconducting transmon qubits are connected to one central computational resonator. In addition to single qubit rotations, all qubits can perform CZ gates with the subspace formed by the two lowest energy levels of the resonator. Furthermore, a MOVE operation is calibrated to exchange the occupations of the qubit-resonator states 0-1 and 1-0. It can therefore be used to shuttle excitations back and forth between any qubit and the resonator [2].

For each number of qubits, 50 random states have been tested and the results are presented in Table 2 and Table 3. In this case, the Hellinger distance between the target probabilities and those achieved by the VQC is computed as the error. With 2 and 3 qubits the results achieved are quite good, but as the number of qubits increases, the performance declines due to the growing complexity of the VQC. However, with IQM Garnet, the error does not increase

significantly and the performance remains good even with more qubits.

n qubit	mean Hellinger distance	std Hellinger distance
2	~ 0.06	~ 0.03
3	~ 0.19	~ 0.09
4	~ 0.36	~ 0.05
5	~ 0.51	~ 0.06

Table 2: Results achieved on IQM Deneb from 2 to 5 qubits.

n qubit	mean Hellinger distance	std Hellinger distance
2	~ 0.03	~ 0.02
3	~ 0.11	~ 0.08
4	~ 0.19	~ 0.04
5	~ 0.31	~ 0.05

Table 3: Results achieved on IQM Garnet from 2 to 5 qubits.

In addition, the network has been tested with specific states. The results are presented in Table 4 for 2-qubit states, Table 5 for 3-qubit states, and Table 6 for 4-qubit states. The results demonstrate that the network can accurately approximate states like uniform superposition, Bell, and GHZ. However, in some cases, the approximation quality significantly decreases.

state	IQM Deneb Hellinger distance	IQM Garnet Hellinger distance
$[1/\sqrt{2}, 0, 0, 1/\sqrt{2}]$ or Bell	~ 0.13	~ 0.12
$[1/\sqrt{2}, 0, 1/\sqrt{2}, 0]$	~ 0.04	~ 0.09
$[0.5, 0.5, 0.5, 0.5]$	~ 0.01	~ 0.01
$[0, 0, 1/\sqrt{2}, -1/\sqrt{2}]$	~ 0.15	~ 0.12
$[-1/\sqrt{2}, 1/\sqrt{2}, 0, 0]$	~ 0.03	~ 0.1

Table 4: Results obtained on IQM Deneb and IQM Garnet using 2 qubits with sparse state or state with a uniform superposition.

4 CONCLUSIONS

In this work, a scalable QNN is proposed to address the state preparation problem in its relaxed version. The parameterized quantum circuit is derived from the traditional QSP ladder structure, redesigned through the Standard Recursive Block Basis (SRBB) decomposition, so as to link the variational parameters to the topology of the Lie group $U(2^n)$ and thus improve its expressiveness and approximation capabilities. Choosing the uniformly controlled gates

state	IQM Deneb Hellinger distance	IQM Garnet Hellinger distance
$[1/\sqrt{2}, 0, 0, 0, 0, 0, 1/\sqrt{2}]$	~ 0.38	~ 0.31
$[0.35, 0.35, 0.35, 0.35, 0.35, 0.35, 0.35, 0.35]$	~ 0.1	~ 0.06
$[1/\sqrt{2}, 1/\sqrt{2}, 0, 0, 0, 0, 0]$	~ 0.23	~ 0.23
$[0, 0, 0, 0, 0, 1/\sqrt{2}, -1/\sqrt{2}]$	~ 0.46	~ 0.25
$[0, 1/\sqrt{2}, 0, 0, 0, -1/\sqrt{2}, 0, 0]$	~ 0.29	~ 0.26

Table 5: Results obtained on IQM Deneb and IQM Garnet using 3 qubits with sparse state or state with a uniform superposition.

state	IQM Deneb Hellinger distance	IQM Garnet Hellinger distance
$[0.25, 0.25, 0.25, 0.25, 0.25, 0.25, 0.25, 0.25, 0.25, 0.25, 0.25, 0.25]$	~ 0.27	~ 0.14
$[0, 0, 0, 0, 0, 0, 0, 0, 0, 0, 0, 0, 0, 1/\sqrt{2}, -1/\sqrt{2}]$	~ 0.74	~ 0.56
$[-1/\sqrt{2}, 1/\sqrt{2}, 0, 0, 0, 0, 0, 0, 0, 0, 0, 0, 0, 0, 0, 0]$	~ 0.33	~ 0.32

Table 6: Results obtained on IQM Deneb and IQM Garnet using 4 qubits with sparse state or state with a uniform superposition.

(UCGs) accordingly, it is possible to use only the diagonal elements of SRBB, reducing the depth by an exponential factor compared to the full algebraic basis and achieving competitive depths and gate counts, in light of algorithmic simplicity and scalability.

The algorithm has been implemented using the PennyLane library, and tests have been performed both with a simulator and with real IQM quantum computers. States of different sizes have been considered, from 2 to 8 qubits with the simulator and from 2 to 5 qubits with the real quantum computer.

The QNN is composed of two components: the first component approximates the modulus of each entry of the target state, while the second component approximates the corresponding phases. Training is then split into two steps; otherwise, the task is more complex and the network cannot achieve good results. Two different optimizers, Adam and Nelder Mead, are considered. With the Adam optimizer, the trace distance and the fidelity are used as loss functions, while when the Nelder-Mead optimizer is chosen, the Frobenius norm is minimized.

Both random states and specific states have been tested. In simulation, the network achieves high accuracy (with errors ranging from 10^{-13} to 10^{-15}) relative to the target state for up to 4 qubits. Accuracy starts to decrease with a higher number of qubits, though the error in the probabilities is within the third or fourth decimal place.

When using IQM hardware, the QNN achieves good results with a small number of qubits when random states are chosen. However, the error is not fixed within a range; instead, it varies significantly depending on the target state. Furthermore, when the target state is the Bell state or a state with a uniform probability distribution, the network achieves a Hellinger distance of around 0.1 with respect to the target state. In contrast, when a different sparse state is used as the target, the QNN produces poor results. The same is observed with 3 qubits: with GHZ and a state with a uniform probability distribution, the QNN achieves a distance of 0.38 and 0.1, respectively, while for other sparse states, the distance increases to 0.6.

In the future, the proposed framework could be compared with well-known QSP algorithms and quantum encoding techniques, such as Amplitude Encoding. Moreover, improving the SRBB synthesis scheme with also the optimization of rotation gates could further reduce the total depth. Another important task is to analyze the landscape, as the network can struggle to achieve high accuracy with a larger number of qubits, due to the increased complexity of the parametric surface, which could lead to the emergence of the Barren Plateaus [27] problem.

ACKNOWLEDGMENTS

Giacomo Belli acknowledges financial support from the European Union - NextGenerationEU, PNRR MUR project PE0000023-NQSTI. Michele Amoretti acknowledges financial support from the European Union - NextGenerationEU, PNRR MUR project CN00000013, Spoke 10, BAC-AQUAMAN. This research benefits from the High Performance Computing facility of the University of Parma, Italy (HPC.unipr.it).

REFERENCES

- [1] Leonid Abdurakhimov, Janos Adam, Hasnain Ahmad, Olli Ahonen, Manuel Algabe, Guillermo Alonso, Ville Bergholm, Rohit Beriwal, Matthias Beuerle, Clinton Bockstiegel, Alessio Calzona, Chun Fai Chan, Daniele Cucurachi, Saga Dahl, Rakhim Davletkaliyev, Olexiy Fedorets, Alejandro Gomez Frieiro, Zheming Gao, Johan Guldmyr, Andrew Guthrie, Juha Hassel, Hermanni Heimonen, Johannes Heinsoo, Tuukka Hiltunen, Keiran Holland, Juho Hotari, Hao Hsu, Antti Huhtala, Eric Hyypä, Aleksi Hämäläinen, Joni Ikonen, Sinan Inel, David Janzso, Teemu Jaakkola, Mate Jenei, Shan Jolin, Kristinn Juliusson, Jaakko Jussila, Shabeeb Khalid, Seung-Goo Kim, Miikka Koistinen, Roope Kokkonieni, Anton Komlev, Caspar Ockeloen-Korppi, Otto Koskinen, Janne Kotilahti, Toivo Kuusma, Vladimir Kukushkin, Kari Kumpulainen, Ilari Kuronen, Joonas Kyllmälä, Niclas Lamponen, Julia Lamprich, Alessandro Landra, Martin Leib, Tianyi Li, Per Liebermann, Aleksi Lintunen, Wei Liu, Jürgen Luus, Fabian Marxer, Arianne Meijer van de Griend, Kunal Mitra, Jalil Khatibi Moqadam, Jakub Mrozek, Henrikki Mäkinen, Janne Mäntylä, Tiina Naaranoja, Francesco Nappi, Janne Niemi, Lucas Ortega, Mario Palma, Miha Papić, Matti Partanen, Jari Penttilä, Alexander Plyushch, Wei Qiu, Aniket Rath, Kari Repo, Tomi Riipinen, Jussi Ritala, Pedro Figueroa Romero, Jarkko Ruoho, Jukka Räbinä, Sampo Saarinen, Indrajit Sagar, Hayk Sargsyan, Matthew Sarsby, Niko Savola, Mykhailo Savitskyi, Ville Selimmaa, Pavel Smirnov, Marcos Marin Suárez, Linus Sundström, Sandra Stupińska, Eelis Takala, Ivan Takmakov, Brian Tarasinski, Manish Thapa, Jukka Tiainen, Francesca Tosto, Jani Tuorila, Carlos Valenzuela, David Vasey, Edwin Vehmaanperä, Antti Vepsäläinen, Aapo Vienamo, Panu Vesanan, Alpo Välimäa, Jaap Wesdorp, Nicola Wurz, Elisabeth Wybo, Lily Yang, and Ali Yurtalan. 2024. Technology and Performance Benchmarks of IQM’s 20-Qubit Quantum Computer. *arXiv:2408.12433* [quant-ph]. <https://arxiv.org/abs/2408.12433>
- [2] Manuel G. Algabe, Mario Ponce-Martinez, Carlos Munuera-Javaloy, Vicente Pina-Canelles, Manish J. Thapa, Bruno G. Taketani, Martin Leib, Inés de Vega, Jorge Casanova, and Hermanni Heimonen. 2022. Co-Design quantum simulation of nanoscale NMR. *Phys. Rev. Res.* 4 (Nov 2022), 043089, Issue 4. <https://doi.org/10.1103/PhysRevResearch.4.043089>
- [3] Israel F Araujo, Daniel K Park, Francesco Petruccione, and Adenilton J da Silva. 2021. A divide-and-conquer algorithm for quantum state preparation. *Scientific reports* 11, 1 (2021), 6329.

[4] Adriano Barenco, Charles H Bennett, Richard Cleve, David P DiVincenzo, Norman Margolus, Peter Shor, Tycho Sleator, John A Smolin, and Harald Weinfurter. 1995. Elementary gates for quantum computation. *Physical review A* 52, 5 (1995), 3457.

[5] Giacomo Belli, Marco Mordacci, and Michele Amoretti. 2024. A Scalable Quantum Neural Network for Approximate SRBB-Based Unitary Synthesis. *arXiv preprint arXiv:2412.03083* (2024).

[6] Giacomo Belli, Marco Mordacci, and Michele Amoretti. 2024. A Scalable Quantum Neural Network for Approximate Unitary Synthesis. In *2024 IEEE International Conference on Quantum Computing and Engineering (QCE)*, Vol. 02, 49–54. <https://doi.org/10.1109/QCE60285.2024.10251>

[7] Marcello Benedetti, Erika Lloyd, Stefan Sack, and Mattia Fiorentini. 2019. Parameterized quantum circuits as machine learning models. *Quantum Science and Technology* 4, 4 (2019), 043001.

[8] Ville Bergholm, Jush Izaac, Maria Schuld, Christian Gogolin, Shahnawaz Ahmed, Vishnu Ajith, M Sohaib Alam, Guillermo Alonso-Linaje, B AkashNarayanan, Ali Asadi, et al. 2018. PennyLane: Automatic differentiation of hybrid quantum-classical computations. *arXiv preprint arXiv:1811.04968* (2018).

[9] Ville Bergholm, Juha J Vartiainen, Mikko Möttönen, and Martti M Salomaa. 2005. Quantum circuits with uniformly controlled one-qubit gates. *Physical Review A—Atomic, Molecular, and Optical Physics* 71, 5 (2005), 052330.

[10] Dmytro Bondarenko and Polina Feldmann. 2020. Quantum autoencoders to denoise quantum data. *Physical review letters* 124, 13 (2020), 130502.

[11] Marco Cerezo, Andrew Arrasmith, Ryan Babbush, Simon C Benjamin, Suguru Endo, Keisuke Fujii, Jarrod R McClean, Kosuke Mitarai, Xiao Yuan, Lukasz Cincio, et al. 2021. Variational quantum algorithms. *Nature Reviews Physics* 3, 9 (2021), 625–644.

[12] David Gosset, Robin Kothari, and Kewen Wu. 2024. Quantum state preparation with optimal T-count. *arXiv preprint arXiv:2411.04790* (2024).

[13] Lov Grover and Terry Rudolph. 2002. Creating superpositions that correspond to efficiently integrable probability distributions. *arXiv preprint quant-ph/0208112* (2002).

[14] Lov K Grover. 2000. Synthesis of quantum superpositions by quantum computation. *Physical review letters* 85, 6 (2000), 1334.

[15] Vu Tuan Hai, Nguyen Tan Viet, and Le Bin Ho. 2023. Variational preparation of entangled states on quantum computers. *arXiv preprint arXiv:2306.17422* (2023).

[16] Jason Iaconis, Sonika Johri, and Elton Yechao Zhu. 2024. Quantum state preparation of normal distributions using matrix product states. *npj Quantum Information* 10, 1 (2024), 15.

[17] Jiaqing Jiang, Xiaoming Sun, Shang-Hua Teng, Bujiao Wu, Kewen Wu, and Jialin Zhang. 2020. Optimal space-depth trade-off of CNOT circuits in quantum logic synthesis. In *Proceedings of the Fourteenth Annual ACM-SIAM Symposium on Discrete Algorithms*. SIAM, 213–229.

[18] Phillip Kaye and Michele Mosca. 2001. Quantum networks for generating arbitrary quantum states. In *International Conference on Quantum Information*. Optica Publishing Group, PB28.

[19] Diederik P Kingma and Jimmy Ba. 2014. Adam: A method for stochastic optimization. *arXiv preprint arXiv:1412.6980* (2014).

[20] Alexander A Kirillov. 2008. *An introduction to Lie groups and Lie algebras*. Vol. 113. Cambridge University Press.

[21] Vadym Kliuchnikov, Alex Bocharov, Martin Roetteler, and Jon Yard. 2015. A framework for approximating qubit unitaries. *arXiv preprint arXiv:1510.03888* (2015).

[22] Vadym Kliuchnikov, Dmitri Maslov, and Michele Mosca. 2012. Fast and efficient exact synthesis of single qubit unitaries generated by Clifford and T gates. *arXiv preprint arXiv:1206.5236* (2012).

[23] Gui-Lu Long and Yang Sun. 2001. Efficient scheme for initializing a quantum register with an arbitrary superposed state. *Physical Review A* 64, 1 (2001), 014303.

[24] Guang Hao Low, Vadym Kliuchnikov, and Luke Schaeffer. 2024. Trading T gates for dirty qubits in state preparation and unitary synthesis. *Quantum* 8 (2024), 1375.

[25] Jingquan Luo and Lvzhou Li. 2024. Circuit complexity of sparse quantum state preparation. *arXiv preprint arXiv:2406.16142* (2024).

[26] Liam Madden and Andrea Simonetto. 2022. Best approximate quantum compiling problems. *ACM Transactions on Quantum Computing* 3, 2 (2022), 1–29.

[27] Jarrod R McClean, Sergio Boixo, Vadim N Smelyanskiy, Ryan Babbush, and Hartmut Neven. 2018. Barren plateaus in quantum neural network training landscapes. *Nature communications* 9, 1 (2018), 4812.

[28] Mikko Möttönen, Juha J Vartiainen, Ville Bergholm, and Martti M Salomaa. 2004. Quantum circuits for general multiqubit gates. *Physical review letters* 93, 13 (2004), 130502.

[29] Mikko Mottonen, Juha J Vartiainen, Ville Bergholm, and Martti M Salomaa. 2004. Transformation of quantum states using uniformly controlled rotations. *arXiv preprint quant-ph/0407010* (2004).

[30] Mikko Möttönen¹ and Juha J Vartiainen. 2006. Decompositions of general quantum gates. *Trends in quantum computing research* (2006), 149.

[31] Fereshte Mozaferi, Giovanni De Micheli, and Yuxiang Yang. 2022. Efficient deterministic preparation of quantum states using decision diagrams. *Physical Review A* 106, 2 (2022), 022617.

[32] Fereshte Mozaferi, Mathias Soeken, Heinz Riener, and Giovanni De Micheli. 2020. Automatic uniform quantum state preparation using decision diagrams. In *2020 IEEE 50th International Symposium on Multiple-Valued Logic (ISMVL)*. IEEE, 170–175.

[33] John A Nelder and Roger Mead. 1965. A simplex method for function minimization. *The computer journal* 7, 4 (1965), 308–313.

[34] Michael A Nielsen and Isaac L Chuang. 2000. *Quantum Computation and Quantum Information*.

[35] Philipp Niemann, Rhitam Datta, and Robert Wille. 2016. Logic synthesis for quantum state generation. In *2016 IEEE 46th International Symposium on Multiple-Valued Logic (ISMVL)*. IEEE, 247–252.

[36] IQM Finland Oy. 2025. IQM website. <https://www.meetiqm.com/>.

[37] Martin Plesch and Časlav Brukner. 2011. Quantum-state preparation with universal gate decompositions. *Physical Review A—Atomic, Molecular, and Optical Physics* 83, 3 (2011), 032302.

[38] Debora Ramacciotti, Andreea I Lefterovici, and Antonio F Rotundo. 2024. Simple quantum algorithm to efficiently prepare sparse states. *Physical Review A* 110, 3 (2024), 032609.

[39] Jonathan Romero, Jonathan P Olson, and Alan Aspuru-Guzik. 2017. Quantum autoencoders for efficient compression of quantum data. *Quantum Science and Technology* 2, 4 (2017), 045001.

[40] Gregory Rosenthal. 2021. Query and depth upper bounds for quantum unitaries via grover search. *arXiv preprint arXiv:2111.07992* (2021).

[41] Yuval R Sanders, Guang Hao Low, Artur Scherer, and Dominic W Berry. 2019. Black-box quantum state preparation without arithmetic. *Physical review letters* 122, 2 (2019), 020502.

[42] Rohit Sarma Sarkar and Bibhas Adhikari. 2023. Scalable quantum circuits for n-qubit unitary matrices. In *2023 IEEE International Conference on Quantum Computing and Engineering (QCE)*, Vol. 1. IEEE, 1078–1088.

[43] Rohit Sarma Sarkar and Bibhas Adhikari. 2024. A quantum neural network framework for scalable quantum circuit approximation of unitary matrices. *arXiv preprint arXiv:2405.00012* (2024).

[44] Vivek V Shende, Stephen S Bullock, and Igor L Markov. 2005. Synthesis of quantum logic circuits. In *Proceedings of the 2005 Asia and South Pacific Design Automation Conference*. 272–275.

[45] Vivek V Shende, Igor L Markov, and Stephen S Bullock. 2004. Minimal universal two-qubit controlled-NOT-based circuits. *Physical Review A—Atomic, Molecular, and Optical Physics* 69, 6 (2004), 062321.

[46] Andrei N Soklakov and Rüdiger Schack. 2006. Efficient state preparation for a register of quantum bits. *Physical Review A—Atomic, Molecular, and Optical Physics* 73, 1 (2006), 012307.

[47] Xiaoming Sun, Guojing Tian, Shuai Yang, Pei Yuan, and Shengyu Zhang. 2023. Asymptotically optimal circuit depth for quantum state preparation and general unitary synthesis. *IEEE Transactions on Computer-Aided Design of Integrated Circuits and Systems* 42, 10 (2023), 3301–3314.

[48] Juha J Vartiainen, Mikko Möttönen, and Martti M Salomaa. 2004. Efficient decomposition of quantum gates. *Physical review letters* 92, 17 (2004), 177902.

[49] Farrokh Vatan and Colin Williams. 2004. Optimal quantum circuits for general two-qubit gates. *Physical Review A—Atomic, Molecular, and Optical Physics* 69, 3 (2004), 032315.

[50] Hanrui Wang, Yilian Liu, Pengyu Liu, Jiaqi Gu, Zirui Li, Zhiding Liang, Jinglei Cheng, Yongshan Ding, Xuehai Qian, Yiyu Shi, et al. 2023. Robuststate: Boosting fidelity of quantum state preparation via noise-aware variational training. *arXiv preprint arXiv:2311.16035* (2023).

[51] Pei Yuan and Shengyu Zhang. 2023. Optimal (controlled) quantum state preparation and improved unitary synthesis by quantum circuits with any number of ancillary qubits. *Quantum* 7 (2023), 956.

[52] Shihao Zhang, Kai Huang, and Lvzhou Li. 2024. Depth-optimized quantum circuit synthesis for diagonal unitary operators with asymptotically optimal gate count. *Physical Review A* 109, 4 (2024), 042601.

[53] Xiao-Ming Zhang, Weicheng Kong, Muhammad Usman Farooq, Man-Hong Yung, Guoping Guo, and Xin Wang. 2021. Generic detection-based error mitigation using quantum autoencoders. *Physical Review A* 103, 4 (2021), L040403.

[54] Xiao-Ming Zhang, Tongyang Li, and Xiao Yuan. 2022. Quantum state preparation with optimal circuit depth: Implementations and applications. *Physical Review Letters* 129, 23 (2022), 230504.

[55] Xiao-Ming Zhang, Man-Hong Yung, and Xiao Yuan. 2021. Low-depth quantum state preparation. *Physical Review Research* 3, 4 (2021), 043200.

[56] Jian Zhao, Yu-Chun Wu, Guang-Can Guo, and Guo-Ping Guo. 2019. State preparation based on quantum phase estimation. *arXiv preprint arXiv:1912.05335* (2019).

[57] Yilun Zhao, Bingmeng Wang, Wenle Jiang, Xiwei Pan, Bing Li, Yinhe Han, and Ying Wang. 2024. SuperEncoder: Towards Universal Neural Approximate Quantum State Preparation. *arXiv preprint arXiv:2408.05435* (2024).